THE PRIMARY COSMIC RAY ELECTRON SPECTRUM NEAR SOLAR MINIMUM*

Jacques L'Heureux+
Enrico Fermi Institute for Nuclear Studies
and Department of Physics
University of Chicago
Chicago, Illinois 60637

Laboratory for Astrophysics and Space Research

EFINS Preprint No. 66-109

November 1966

(To be published in May 1967 issue of the
Astrophysical Journal)

* This research was supported in part by the National Aeronautics and Space Administration under Grant No. NASA-NsG 144-61 Res. and by the National Science Foundation under Grant No. GP-4709.

+ A thesis submitted to the Department of Physics, the University of Chicago, Chicago, Illinois, in partial fulfillment of the requirements for the Ph.D. degree.

THE PRIMARY COSMIC RAY ELECTRON SPECTRUM NEAR SOLAR MINIMUM*

Jacques L'Heureux+
Enrico Fermi Institute for Nuclear Studies
and Department of Physics
University of Chicago
Chicago, Ill. 60637

ABSTRACT

Two balloon flights were made from Fort Churchill, Manitoba in the summer of 1965, to continue our investigation of the flux and energy spectrum of the primary cosmic ray electron component. The spectrum was studied for energies from 20 MeV to 5.5 BeV. Above 1.2 BeV, the differential energy spectrum can be represented by a power law of the form $dJ/dE = (48 \pm 15)E^{-(2.1 \pm 0.3)}$ electrons/m^2 sec ster BeV. For energies below 1 BeV, the spectrum becomes flatter (slope $\gamma \lesssim 1.6$). Between 20 MeV and 270 MeV, the total flux rather than the differential flux has been measured. Its value is 180 ± 30 electrons/m^2 sec ster. A comparison of our results with data at higher energies obtained by other authors indicates that the spectrum is steeper above 10 BeV ($\gamma = 2.45$).

Our data are also compared with the results obtained from the observations of the nonthermal radio emission from high galactic latitudes. The electron energy spectrum obtained in this experiment is, for energies greater than

---

* This research was supported in part by the National Aeronautics and Space Administration under Grant No. NASA-NsG 144-61 Res. and by the National Science Foundation under Grant No. GP-4709.

+ A thesis submitted to the Department of Physics, the University of Chicago, Chicago, Illinois, in partial fulfillment of the requirements for the Ph.D. degree.

1 BeV, in agreement with the spectrum of galactic electrons as derived from the radio noise measurements. Below 1 BeV, the measured electron energy spectrum is flatter than would be predicted on the basis of the radio noise frequency spectrum for frequencies less than 50 Mc/sec (corresponding to electrons below 1 BeV). This might be an indication that solar modulation, even near solar minimum, affects the electron spectrum measured at the earth.

The measurements were carried out using a counter system. A total absorbtion lead glass Cerenkov counter was used to obtain the energy of the electrons. Low energy protons were rejected by the use of a gas Cerenkov threshold counter. Guard counters served to identify high energy protons.

I. Introduction

The search for the primary electron component in the cosmic radiation began as early as 1941 (Schein, Jesse, and Wolland 1941). In the following years, two experiments yielded upper limits for the electron flux (Hulsizer and Rossi 1948; Critchfield, Ney and Oleksa 1952). The cloud chamber experiment of Critchfield et al. gave an upper limit for the flux of the primary electrons of 0.6% of the total cosmic ray flux. Two experiments carried out in 1960 led to the identification of primary electrons and permitted a rough measurement of their flux. Earl (1961) has reported a flux of primary electrons between 500 MeV and 3 BeV amounting to (3 ± 1) % of the flux of the minimum ionizing primary cosmic ray protons. Meyer and Vogt (1961a) have observed a significant flux of electrons with energies between 25 MeV and 1.3 BeV.

The first evidence for the existence of relativistic electrons in the galaxy came from observations of the galactic radio noise and from the interpretation that this nonthermal radio emission was due to synchroton radiation by high energy electrons in the magnetic fields of the galaxy (Kiepenheuer 1950). Kiepenheuer's order of magnitude calculation showed that the required electron flux in the galaxy was not in disagreement with the upper limits reported in the early search for primary electrons. Hayakawa (1952) postulated that the relativistic electrons in the galaxy originated in the decay of π-mesons produced by cosmic ray proton interactions with the interstellar gas. He concluded that an electron to proton flux ratio of 1% is consistent with a total path length for the protons in the galaxy of 3 g/cm^2 of hydrogen. A more refined calculation of the flux and energy spectrum of collision produced electrons was made by Hayakawa and Okuda (1962). Their results were shown to be in fair agreement

with the flux measured by Earl (1961) and by Meyer and Vogt (1961a).

In recent years, more detailed measurements of the integral and of the differential electron energy spectrum have been performed (Agrinier, Koechlin, Parlier, Boella, DegliAntoni, Dilworth, Scarsi, and Sironi 1964; Agrinier, Koechlin, Parlier, Vasseur, Bland, Boella, DegliAntoni, Dilworth, Scarsi, and Sironi 1965; Bleeker, Burger, Sheepmaker, Swanenburg, and Tanaka 1965; Cline, Ludwig, and McDonald 1964; Daniel and Stephens 1965; Freier and Waddington 1965; L'Heureux and Meyer 1965; Schmoker and Earl 1965). These measurements cover various energy regions: 3 MeV to 12 MeV, 45 MeV to 150 MeV and also above 500 MeV. In the light of these recent experiments, the hypothesis of the origin of the electrons in the galactic p-p collisions (collision hypothesis) has been re-examined (Ginzburg and Syrovatskii 1964; Ramaty and Lingenfelter 1966). It has become evident from the experimental results that the collision hypothesis cannot account for the observed electron intensity and energy spectrum, at least for electron energies above 1 BeV. This conclusion has also been reached independently as a result of the observation of the large negative excess in the charge composition of the primary electron component (Bland, Boella, DegliAntoni, Dilworth, Scarsi, Sironi, Agrinier, Koechlin, Parlier and Vasseur 1966; DeShong, Hildebrand and Meyer 1964; Hartman, Meyer and Hildebrand 1965; Hartman 1966).

In this paper, we shall present results which were obtained during two balloon flights in 1965 with a detector system nearly identical to the one which we used in 1964 (L'Heureux and Meyer 1965). The range now covered by the instrument extends from 20 MeV to 5.5 BeV (primary energy). We shall present

a detailed energy spectrum above 270 MeV. Below that energy, only the integral flux can be measured (20 MeV to 270 MeV). The primary electron flux below 500 MeV is difficult to study at balloon altitude because of the large contribution of atmospheric secondary electrons to the measured flux. Attempts were made to improve the methods of correction for secondary electrons in order to arrive at a primary electron energy spectrum. The accuracy of the results in the low energy region strongly depends on the accuracy of the method of correction.

The energy spectrum which was obtained in this experiment permits a detailed comparison with predictions for the electron flux and energy spectrum on the basis of various hypotheses. It also permits a comparison with the results obtained from the observations of the nonthermal radio emission in the galaxy.

II. INSTRUMENTATION

A. The Detector System

Figure 1 shows a schematic cross-section of the detector system which was used in this experiment. Vertically incident particles are selected using coincidences from a counter telescope formed by the thin plastic scintillator counter I and from a second plastic scintillator counter T. The acceptance of an event also requires the triggering of the gas Cerenkov counter C located in the counter telescope. This gas Cerenkov counter is filled with SF_6 ($n - 1 = 7.83 \times 10^{-4}$ at STP) at an absolute pressure of 2.3 atm., and is sensitive to charged particles having a total energy greater than 20 times their rest energy. Therefore, the energy threshold of our system for electrons, protons, and alpha particles is 10 MeV, 18 BeV and 18 BeV/nucleon respectively. The counter system therefore

efficiently discriminates against the large flux of low energy protons present in the primary cosmic radiation. The geometry factor of the system is 1.08 cm^2 ster.

Counter I defines the geometry of the telescope and is also used for an energy loss measurement (dE/dx) of the entering particles. Since all accepted particles are highly relativistic, this measurement makes it possible to sort them according to their charge. The particles will then enter the lead glass Cerenkov detector II. This counter, consisting of a 20 cm deep cylinder of lead glass (Schott SF6-FA, η = 1.80, density = 5.10 g/cm^3 , radiation length = 1.49 cm), is optically coupled to a 12.7 cm photomultiplier tube. In the lead glass, an electron will develop an electron-photon shower. Provided that the shower is confined in the lead glass cylinder, the total amount of Cerenkov light produced will be roughly proportional to the energy of the entering electron.

We must discriminate against those protons with energy greater than 18 BeV which, upon interaction in the lead glass, may produce π^o mesons and consequently an electron shower. The A3 guard counter is used to reject all of the proton events which contain at least one downward moving charged secondary. The few events caused by interacting protons in which the A3 counter is not fired are discriminated against by the counter S. This counter is placed under a disk of lead, 10.8 g/cm^2 thick and directly above the lead glass Cerenkov counter. The pulse from the counter S is directed to two independent discriminators. The discriminator S1 will respond to particles having minimum ionization or more. The discriminator S2 responds only if the total energy loss in the counter is more than

1.6 times the average loss of a relativistic, singly charged particle. For a singly charged particle accepted by the counter telescope the triggering of the S2 discriminator means in 80% of the cases that the particle has interacted in the lead disc and that two or more particles emerged from it. Because of the statistical fluctuations of the energy loss in counter S, 20% of the singly charged particles accepted by the counter telescope will trigger S2. This counter will therefore permit removal of 80% of those proton events for which A3 was not fired.

To reject showers produced in the gondola shell material or in the counter I, the anticoincidence counter A1 covers the top of the lead glass Cerenkov counter II except for a hole in the center. For convenience, the disc of lead mentioned above fills that hole. Another guard counter (A2) surrounds the counter II. Like A3, it indicates the leakage of one or more particles out of the lead glass counter II.

The entire detector system has been calibrated in a monoenergetic beam of electrons at energies ranging from 700 MeV to 4 BeV. The results of the calibration will be discussed in section III-C.

B. The Logic System

The data which are collected during a flight are immediately transformed into a digital form suitable for on-board recording, and for transmitting to the ground. For the on-board recording, we have used a 6-channel tape recorder with a tape speed of 1 cm/sec. This permits the collection of data for a flight of 20 hours duration on 2400 ft (731 m) of 1/2-mil thick mylar recording tape. The digital data are simultaneously transmitted to a ground receiving and recording station.

Six subcarriers modulate a 73 Mc/sec FM transmitter via Pulse-Code-Modulation. Figure 2 represents the airborne analysis system. A triple coincidence between the counters T, C, and I not accompanied by A1 starts the analysis. The pulse height from the energy loss counter is analyzed by a 32 channel pulse height analyzer, while counter II is being read by a 128 channel analyzer. For each event, the state of the discriminators S1, S2, A2 and A3 is indicated. Once a minute, for a nominal period of 2 seconds, data from a coincidence register, temperature sensor, and from an aneroid-type pressure transducer are transmitted.

During the flights, the equipment is housed in a cylindrical aluminum container sealed at a pressure of 1 atm. A thermostat controlled heater maintains the equipment temperature between 7° C and 20° C.

C. The Flights

Our results were obtained from two balloon flights, launched on June 25 and July 16, 1965 from Fort Churchill, Canada. In each flight, the detector system floated for 13 hours at an average atmospheric depth of 3.8 and 5.0 g/cm^2 respectively. Fort Churchill (72.8° N geomagnetic latitude) has a calculated vertical threshold rigidity of 186 MV (Quenby and Wenk 1965). However, there has been experimental evidence (Stone 1964) that for geomagnetic latitudes above 65° the cut-off is less than 55 MV (1.5 MeV for protons). Recently, Michel (1965) and Reid and Sauer (1966) argue that due to the existence of a geomagnetic tail, the effective threshold might be well below this value, possibly less than 10 MV for geomagnetic latitudes above 65° - 70° N. On this basis, we will consider all vertically incident electrons with energies greater than 20 MeV as primaries rather than return albedo electrons.

III. DATA ANALYSIS AND CORRECTIONS

A. Rejection of High Energy Protons and the Identification of the Electrons

The energy loss measurement performed by the scintillation counter I permits the separation of protons and electrons from multiply charged particles. For low energy electrons, the electron photon shower will be completely contained in the lead glass counter II. Higher energy electrons will produce showers which will be detected by the guard counters (A2 and/or A3). Since the lead glass counter II has a radius of only 4.2 radiation lengths compared to a depth of 13 radiation lengths, large showers have a higher probability to fire the A2 guard counter than A3. In our range of electron energies, except for a small correction for protons, all of the events that do not fire A3 (symbolized by $\overline{A3}$) are caused by electrons whether A2 has been fired or not. The corrections to the $\overline{A3}$ electron events are:

i) The gas Cerenkov is completely insensitive to protons of energy below its threshold (18 BeV). A small fraction of low energy protons (0.1%) is accepted by chance coincidence with the gas Cerenkov random noise pulses. We shall point out later how we can experimentally determine that these cosmic ray protons cannot contribute more than a few percent of the $\overline{A3}$ electron events.

ii) The accepted high energy protons (> 18 BeV) can also simulate an $\overline{A3}$ electron event. But to do so, they must interact in the lead glass and not produce any downward moving charged secondaries which could fire A3. This is a very unlikely event as confirmed by our observations which are described in section IV-A.

B. Corrections for Atmospheric Secondary Electrons

In the energy region of interest, the contribution by atmospheric secondary electrons to the total electron flux at balloon altitude is appreciable. Under 3 to 4 g/cm^2 of atmosphere, this contribution to the electron flux above 700 MeV amounts to 11%. The correction for secondaries becomes increasingly large below that energy. We have approached the problem of secondary correction by two different although not entirely independent methods:

i) The processes by which secondary electrons are produced in the atmosphere are well known. On the basis of new experimental data on high energy production cross sections of pions, the secondary electron flux and energy spectrum have been computed by Perola and Scarsi (1966) and by Verma (1966). The calculation of Verma (1966) will be used later to correct our data.

ii) The second method uses the experimental data on the secondary electrons obtained during the ascent of the equipment through the atmosphere. Since at depths larger than about 20 g/cm^2, the electron flux consists mostly of secondaries, we can extrapolate the measured electron flux to smaller depths. The shape of the extrapolation curve is known from simple considerations of the processes involved in the production of these secondary electrons (Verma 1966).

In section IV. B., these two methods of correction will be applied to the data.

C. Calibration of the Detectors

A calibration of our detector system has been carried out in a monoenergetic, well collimated beam of electrons at energies ranging from

700 MeV to 4 BeV.[1] We have calibrated the lead glass Cerenkov counter up to an energy of 2.1 BeV. (The pulse height analyzer used at the time of the calibration saturated at that energy.) The energy resolution of this detector was measured to be 32% (full width at half maximum) at 700 MeV, 21% at 1.3 BeV and 11% at 2.1 BeV. The efficiency of the gas Cerenkov counter for highly relativistic electrons was measured to be (95 $\pm$ 2)%. Within the accuracy of the measurement, it was found to be independent of the angle of incidence of the particle for angles within 15° of the telescope axis. Our telescope accepts only particles within 11° of the telescope axis. The efficiency of the gas Cerenkov detector was independently derived using the pulse height distribution of Cerenkov pulses from cosmic ray muons and the knowledge of the discriminator level. It is in agreement with the directly measured efficiency.

[1]We wish to express our gratitude to Dr. M. S. Livingston for making a beam of the Cambridge electron accelerator available to us and to Dr. M. Fotino, Dr. L. N. Hand and Dr. E. Engels for their help in setting up our experiment.

The fraction of events for which the counter A3 was fired was obtained for various electron energies using the accelerator beam. A similar study was made to measure the fraction of the events for which only one particle traversed the shower counter S. These data will be used later (IV, A) to correct the observed electron flux.

IV. RESULTS

A. Electron Flux and Energy Spectrum at 4.4 g/cm^2

During each of the two balloon flights, 13 hours of continuous data

were collected at average floating altitudes of 3.8 and 5.0 g/cm^2 respectively. In addition, 4 hours of data were collected during the ascents of the equipment. These were used to construct the growth curves (flux vs. atmospheric depth). Inflight calibration of the lead glass Cerenkov detector by highly relativistic protons as well as pre-flight ground runs with cosmic ray muons are used to accurately determine the energy scale of counter II. The data must then be corrected for the contribution of protons. As was mentioned earlier, the events for which the guard counter A3 has not been fired are considered electrons except for a small contribution of protons. In figure 3, we have plotted, as a function of energy, the fraction of the $\overline{A3}$ events for which the shower counter detected only one particle (S1 type) for both A2 and $\overline{A2}$ events. The solid line represents this probability in the case of a pure electron beam. The high energy portion of the curve is obtained from the electron accelerator measurements and for energies below 0.7 BeV from a calculation of the shower development in lead (Nagel 1965). These data show that, within the accuracy of the measurement, protons are not contributing at all to the $\overline{A2}\,\overline{A3}$ electron events. For the $A2\,\overline{A3}$ type electron events (with side leakage), a contribution of protons can be observed only in the 2 - 4.9 BeV energy range. In that range, it appears that protons contribute $(14 \pm 11)\%$ of the events, which means that 2 of the 14 $A2\overline{A3}$ type events are more likely to be protons that have interacted in the lead glass counter, than electrons.

The most important correction which we must apply to the data involves the probability that a shower produced in the lead glass counter will not fire the A3 guard counter. This probability strongly depends on energy. At high

energies, where the probability is largest, a correction factor is derived from the electron beam calibration and, for energies below 700 MeV, from calculations on the shower development in lead (Nagel 1965). As an example, this probability amounts to 95% at 400 MeV and to 22% at 3 BeV.

The probability that particles from a shower trigger the anti-coincidence guard counter A1 must also be taken into account. We have used the lateral distribution of showers in lead (Nagel 1965) and obtained a correction factor. It amounts to 10 ± 5 % and is approximately independent of energy.

Finally, corrections were applied to take care of the efficiency of the gas Cerenkov counter and of the dead time of the logic circuits. Both these corrections are independent of particle energy and each amounts to 5%.

We have combined the results of the two flights using all 26 hours for which data were collected. The average atmospheric depth was 4.4 g/cm^2. The total electron energy spectrum (primary plus atmospheric secondary) measured at that depth is shown in figure 5.

B. The Primary Electron Flux and Energy Spectrum

We will now consider the contribution of atmospheric secondaries and extrapolate the spectrum to the top of the atmosphere to obtain the primary electron energy spectrum. We may point out here that no distinction between electrons and positrons is made.

To correct for atmospheric secondaries, we have adopted a mixture of the two methods mentioned earlier. We have divided all the data which were collected during the ascents of the two balloon flights into 4 energy groups. Figures 4a), b), c) and d) show how the flux of electrons in each energy interval

varies as a function of atmospheric depth. The solid curve represents the flux of secondary electrons. Its slope is derived from the calculation of Verma (1966) but the intensity has been normalized to the interpolated measured flux at a depth of approximately 20 g/cm^2. The dot-dashed curve shows how the primary flux in each energy interval decreases with depth due to ionization and bremstrahlung losses in the atmosphere. The dashed curve is the sum of these two contributions which, in all energy intervals, fits the data rather well at atmospheric depths below 20 g/cm^2. It is normalized at 4.4 g/cm^2 to the measured data. As mentioned earlier, the secondary electron spectrum at 4.4 g/cm^2 has been calculated by Verma (1966). The spectrum that resulted from his work is shown in figure 5 (curve b). Over each of the energy intervals of interest, we have integrated this secondary electron spectrum calculated for a depth of 4.4 g/cm^2 and compared it with the extrapolated secondary flux. In the energy region 10 - 230 MeV, it is in perfect agreement with the measured flux extrapolation. In the other three energy intervals, the extrapolated secondary electron flux is slightly lower than the calculated one. We have then modified the calculated secondary spectrum in such a way that the flux in each energy interval agreed with the experimentally extrapolated flux. In this way, we arrived at a semi-empirical secondary spectrum (curve a in figure 5). This semi-empirical spectrum has been used for corrections and it is in agreement with the calculated spectrum which was estimated to be only accurate within $\pm$ 25% (Verma 1966).

The primary electron spectrum at a depth of 4.4 g/cm^2 is derived by subtracting the semi-empirical electron spectrum (curve (a) in figure 5) from

the measured total electron spectrum. This primary spectrum is extrapolated to the top of the atmosphere by making corrections for ionization and bremsstrahlung losses in the air above the detector. No corrections were made for energy losses in the entrance window and in the telescope counters of the detector system since the energy calibrations on the electron accelerator were carried out with an equivalent amount of material in the counter telescope. The primary electron spectrum which we obtain after these corrections is shown in figure 6. The energy region from 20 MeV to 270 MeV (10-230 MeV at the level of the balloon) has not been included in the energy spectrum. In this energy interval, the corrected primary flux is found to be 180 ± 30 electrons/m^2 sec ster.

At energies above 1.2 BeV the spectrum can be represented by a power law of the form

$$dJ/dE = (48 \pm 15)\, E^{-(2.1 \pm 0.3)} \text{ electrons/m}^2 \text{ sec ster BeV}$$

for $1.2 \text{ BeV} < E < 5.5 \text{ BeV}$.

The spectrum becomes flatter below 1.2 BeV.

C. Time Variations

In the summer of 1964, we had carried out an experiment with an almost identical detector system. The electron intensity reported from that experiment (L'Heureux and Meyer 1965) is lower than the one presented here. The use of a smaller correction in the analysis of the 1964 data is responsible for this difference. The analysis of the 1965 results made it clear that we had underestimated the probability for an electron photon shower to trigger the side guard counter A2. Using a new correction factor which we obtained from this year's data and also the

improved secondary electron spectrum, we have recalculated the 1964 primary electron energy spectrum. The range has been extended on the low energy side. The recorrected 1964 spectrum is compared in figure 7 with the 1965 spectrum. A power law fit to the three 1964 data points above 0.77 BeV can be written as

$$dJ/dE = (28 \pm 12)\, E^{-(2.0 \pm 0.5)} \text{ electrons/m}^2 \text{ sec ster BeV}$$

for $0.77 \text{ BeV} < E < 3.6 \text{ BeV}$.

The two spectra taken a year apart are in good agreement with each other. A substantial change in intensity is not expected from 1964 to 1965 since the Deep River neutron monitor (Steljes 1965) shows that the cosmic ray intensity in both the summers of 1964 and 1965 is within 3% of the maximum intensity recorded around April - May 1965. Therefore the 1965 spectrum presented here can be considered representative for the primary electrons at the earth during the minimum of solar activity.

D. Comparison with Other Investigations

In figure 8, we have summarized all recent measurements of the primary electron differential energy spectrum. Included with our results are those of Cline et al. (1964) at low energies and the high energy results of Bleeker et al. (1965) and of Daniel and Stephens (1965). Our results are in very good agreement with those of Bleeker et al. (1965) in the energy region in which they overlap. All results shown are either free from a contribution of atmospheric secondaries or have been corrected for it. Above 1.85 BeV, a power law was fitted to the spectrum by the least squares method. The fit between 1.85 BeV and 355 BeV shown by the solid line in figure 9 can be represented by

$$\frac{dJ}{dE} = (60 \pm 18)\, E^{-(2.45 \pm 0.20)} \text{ electrons/m}^2 \text{ sec ster BeV}$$

$$1.85 \text{ BeV} < E < 355 \text{ BeV}$$

In the restricted range from 1.85 BeV to 15 BeV the spectrum is best represented by

$$\frac{dJ}{dE} = (46 \pm 18)\, E^{-(2.2 \pm 0.3)} \text{ electrons/m}^2 \text{ sec ster BeV}$$

$$1.85 \text{ BeV} < E < 15 \text{ BeV}$$

A comparison of these fits with the one discussed in IV-B seems to indicate a slowly steepening spectrum toward higher energies.

V. CONCLUSIONS

Origin of the electrons. The galactic origin of the primary electrons was first postulated by Hayakawa (1952) on the basis of p-p collisions. Ramaty and Lingenfelter (1966) have recently recalculated the equilibrium spectrum of galactic electrons produced by high energy collisions in galactic space. They have taken account of proton-proton, proton-helium and alpha-proton collisions as well as neutron decay. Their results are shown by the dot-dashed curve in figure 8. This calculation is for the case of a halo magnetic field intensity of 3×10^{-6} gauss and a photon energy density of 0.1 ev/cm^3. The average amount of material traversed by the cosmic rays to produce the spectrum shown is 3 g/cm^2.

It is immediately obvious that for energies above approximately 1 BeV, the secondary hypothesis fails to supply a sufficient number of electrons to explain the observed spectrum at the earth. Earl (1961) was the first to point out this discrepancy when he measured the primary electron flux above a latitude

cutoff of 0.7 BV. A study of the positron-electron ratio in the cosmic radiation has provided more direct evidence pointing in this direction. For energies above 1 BeV, instead of the positron excess predicted by the collision hypothesis (see Ramaty and Lingenfelter (1966)), Hartman, Meyer and Hildebrand (1965) and Hartman (1966) have observed that the electrons outnumber the positrons at least 2 to 1. From these results they concluded that only part of the primary electron component of the cosmic radiation originates in p-p collisions. These excess negative electrons may have been directly accelerated in supernova remnants (Ginzburg 1958).

In the 100 MeV to 1 BeV energy region, our measured spectrum tends to agree with the calculated galactic secondary spectrum. The collision hypothesis,however, predicts for that energy region a large positron excess. But the results of DeShong et al. (1964), of Hartman et al. (1965) and of Hartman (1966) show that also in the energy region from 100 MeV to 1 BeV, there are still more electrons than positrons (possibly 2 to 1). We are then led to believe that the electron flux below 1 BeV as observed at the orbit of the earth, is lower than the galactic electron flux. Since solar modulation of primary electrons has been observed before[1], it may account for a reduced electron flux,

---

[1] During a Forbush-type decrease in 1960, Meyer and Vogt (1961b) have observed the electron flux in the energy range 100 MeV to 1 BeV to decrease by 40% while the proton flux above 350 MeV decreased by 9%.

---

even near solar minimum. We will see some more evidence later pointing to this effect.

A calculation of the energy spectrum of knock-on electrons produced in the galaxy was carried out by Abraham, Brunstein and Cline (1966). Their result is shown in figure 8 by the dashed line. The knock-on process produces a significant intensity in the low energy region which is, however, too small to explain the observations.

It is illustrative to construct an integral spectrum of the primary electrons. The spectrum shown in figure 9 was obtained in the following way. The results of Bleeker et al. (1965) have been added to the results of Daniel and Stephens (1965) to form an integral spectrum down to 2 BeV. Our results were added to the integral flux above 5.5 BeV and the integral spectrum extended to 270 MeV. A similar procedure was used with the results of Earl (1961). The other data are directly measured integral fluxes. For energies larger than 1.85 BeV, a power law spectrum was fitted by the least squares method giving the following flux

$$J\,(<E) = (51 \pm 12)\, E^{-(1.44 \pm 0.16)} \text{ electrons/m}^2 \text{ sec ster}$$

Above 2 BeV, this flux represents about 0.7% of the proton flux as published by Ormes and Webber (1965).

On the same graph, we have also drawn the integral intensity on the basis of the galactic collision hypothesis. It was obtained by integrating the differential energy spectrum derived by Ramaty and Lingenfelter (1966) with the added assumption that the differential spectrum continues to high energies with a power law having an exponent of -3.1. This flux for collision electrons is an upper limit since this extrapolation to high energies neglects synchrotron losses. at 1 BeV, the prediction of the collision hypothesis is an order of magnitude too low, and, above 10 BeV, it explains no more than 4% of the observed flux.

Galactic radio noise. The nonthermal radio noise background that is observed in the direction of the galactic poles is believed to be due to synchrotron emission by relativistic electrons. Wielebinski and Yates (1965) have summarized these radio noise results. In the frequency range 18 - 400 Mc/sec (corresponding to electron energies from 600 MeV to 3.5 BeV), the frequency spectral index was found to be $\alpha = .65 \pm .15$. If the spectrum of the electrons responsible for the radio emission is assumed to be of the form

$$\frac{dJ}{dE} = K E^{-\gamma}$$

the radio noise results imply that the slope of the electron energy spectrum should be

$$\gamma = 2\alpha + 1 = 2.3 \pm 0.3.$$

Above 1 BeV, this is in agreement with our results. In the 600 MeV to 1 BeV range, the slope of the energy spectrum as measured at the earth is flatter than the one inferred by the galactic radio noise measurements. This change in slope below 1 BeV in the measured electron spectrum without a similar flattening of the radio noise frequency spectrum below 50 Mc/sec seems to indicate that even near solar minimum, the electron flux below 1 BeV observed at the orbit of earth is lower than the flux outside of the solar system. This fact has been noted before (Felten 1966).

The measured electron flux above energies of 1 BeV is now in fairly good agreement with the intensity derived from the radio observations. A discrepancy which was suggested on the basis of our earlier observations (Meyer 1965) does no longer exist. The connection between the galactic nonthermal radio emission and the observed electron fluxes has recently been discussed in some detail by Felten (1966).

Acknowledgments. The author wishes to thank his faculty sponsor, Professor Peter Meyer, for suggesting this problem, for many helpful discussions, and for continued support throughout the time this work was in progress. We are indebted to Mssrs. T. Burdick and H. Boersma for their invaluable help in the electronics work, to Mssrs. W. Johnson, A. Hoteko and S. Avery for their participation in the development and construction of the equipment. Many thanks are due to Mssrs. R. Eckstrom and L. Hecht for their help in the data analysis. We gratefully acknowledge the support given to us by the Skyhook program of the Office of Naval Research and by the Royal Canadian Air Force at Fort Churchill, Manitoba.

REFERENCES

Abraham, P. B., Brunstein, K. A., and Cline, T. L. 1966, Energetic Particles Preprint Series, No. X-611-66-57.

Agrinier, B., Koechlin, Y., Parlier, B., Boella, G., DegliAntoni, G., Dilworth, C., Scarsi, L., and Sironi, G. 1964, Phys. Rev. Letters 13, 377.

Agrinier, B., Koechlin, Y., Parlier, B., Vasseur, J., Bland, C. J., Boella, G., DegliAntoni, G., Dilworth, C., Scarsi, L., and Sironi, G. 1965, in Proceedings of the Ninth International Conference on Cosmic Rays, Vol. 1, 331 (London: The Institute of Physics and the Physical Society).

Bland, C. J., Boella, G., DegliAntoni, G., Dilworth, C., Scarsi, L., Sironi, G., Agrinier, B., Koechlin, Y., Parlier, B., and Vasseur, J. 1966, Phys. Rev. Letters 15, 813.

Bleeker, J. A. M., Burger, J. J., Sheepmaker, A., Swanenburg, B. N., and Tanaka, Y. 1965, in Proceedings of the Ninth International Conference on Cosmic Rays, Vol. 1, 327 (London: The Institute of Physics and the Physical Society).

Cline, T. L., Ludwig, G. H., and McDonald, F. B. 1964, Phys. Rev. Letters 13, 786.

Critchfield, C. L., Ney, E. P., and Oleksa, S. 1952, Phys. Rev. 85, 461.

Daniel, R. R., and Stephens, S. A. 1965, Phys. Rev. Letters 15, 769.

DeShong, J. A., Jr., Hildebrand, R. H., and Meyer, P. 1964, Phys. Rev. Letters 12, 3.

Earl, J. A. 1961, Phys. Rev. Letters 6, 125.

Felten, J E. 1966, Ap. J., 145, 589.

Freier, P. S., and Waddington, C. J. 1965, J. Geophys. Research 70, 5753.

Ginzburg, V. L. 1958, in Progress in Elementary Particle and Cosmic Ray Physics, Vol. 4 (North-Holland Publishing Company, Amsterdam).

Ginzburg, V. L., and Syrovatskii, S. I. 1964, The Origin of Cosmic Rays (New York: Pergamon Press).

Hartman, R. C., Meyer, P., and Hildebrand, R. H. 1965, J. Geophys. Research 70, 2713.

Hartman, R. C. 1966 (to be published).

Hayakawa, S. 1952, Prog. Theor. Phys. 8, 571.

Hayakawa, S., and Okuda, H. 1962, Prog. Theor. Phys. 28, 517.

Hulsizer, R. I., and Rossi, B. 1948, Phys. Rev. 73, 1402.

Kiepenheuer, K. O. 1950, Phys. Rev. 79, 738.

L'Heureux, J., and Meyer, P. 1965, Phys. Rev. Letters 15, 93.

Meyer, P. 1965, in Proceedings of the Ninth International Conference on Cosmic Rays, Vol. 1, 61 (London: The Institute of Physics and the Physical Society).

Meyer, P., and Vogt, R. 1961a, Phys. Rev. Letters 6, 193.
_____ 1961b, J. Geophys. Research, 66, 3950.

Michel, F. C. 1965, Planet. Space Sci. 13, 753.

Nagel, H. H. 1965, Z. Phys., 186, 319.

Ormes, J. F., and Webber, W. R. 1965, in Proceedings of the Ninth International Conference on Cosmic Rays, Vol. 1, 349 (London: The Institute of Physics and the Physical Society).

Perola, G. C., and Scarsi, L. 1966, Preprint.

Quenby, J. J., and Wenk, G. T. 1962, Phil. Mag. 7, 1457.

Ramaty, R., and Lingenfelter, R. E. 1966, J. Geophys. Research 71, 3687.

Reid, G. C., and Sauer, H. H. 1966 (Preprint)

Rubtsov, V. I. 1965, in Proceedings of the Ninth International Conference on Cosmic Rays, Vol. 1, 324 (London: The Institute of Physics and the Physical Society).

Schein, M., Jesse, W. P., and Wollan, E. O. 1941, Phys. Rev. 59, 615.

Schmoker, J. W., and Earl, J. A. 1965, Phys. Rev. 138, B300.

Steljes, J. F. 1965, Atomic Energy of Canada Limited, Publication No. AECL-2513.

Stone, E. C. 1964, J. Geophys. Research 69, 3577.

Verma, S. D. 1966 (Submitted for publication)

Wielebinski, R., and Yates, K. W. 1965, Nature 205, 581.

Figure Captions

Figire 1 Schematic cross section of the detector system.

Figure 2. Block diagram of the airborne electronic system.

Figure 3. Probability for an electron which is accepted by the detector system to produce an event of the type S1, as a function of energy (see section IV-A). The solid curve was derived partly from measurements on an accelerator beam and partly from a calculation. The data points represent the fraction of the events for which the trigger S1 was fired. These data were collected at floating altitude.

Figure 4a) b)c)d) The measured vertical electron flux as a function of atmospheric depth for electrons in different energy ranges. The solid line represents the calculated flux of atmospheric secondary electrons vs. atmospheric depth. The dot-dashed curve is the calculated primary flux (normalized at 4.4 g/cm^2) as a function of depth. The sum of these two contributions is shown by the dashed curve and, below 20 g/cm^2, should be compared with the measured electron flux.

Figure 5 The total electron flux (primary plus secondary) as measured at an average depth of 4.4 g/cm^2 in the atmosphere. Curve (b) is a calculated energy spectrum of the atmospheric electrons (Verma 1966). Curve (a) is a semi-empirical secondary energy spectrum used to correct our data (see section IV-B).

Figure 6 The primary electron energy spectrum extrapolated to the top of the atmosphere as measured in 1965.

Figure 7 The primary electron energy spectrum measured in 1965, compared with the modified results of 1964.

Figure 8 The differential energy spectrum of the primary electrons from recent experiments. A least squares fit including all data above 1.5 BeV gives $dJ(E)/dE = (60 \pm 18)\ E^{-(2.45 \pm 0.20)}$ electrons/ (m^2 sec ster BeV) and is shown by the solid line. The dashed curve is the spectrum calculated by Abraham et al. (1966). for galactic knock-on secondaries. The dot-dashed curve represents the calculated equilibrium energy spectra of electrons produced by cosmic ray interactions in the galaxy. (Ramaty and Lingenfelter 1966.)

Figure 9 The integral spectrum of primary electrons in the energy region from 300 MeV to 300 BeV. The differential measurements (indicated by an asterisk) are normalized to the integral flux at the highest energy. A least squares fit to the data for energies above 1.5 BeV yields $J(>E) = (51 \pm 12)\ E^{-(1.44 \pm 0.16)}$ electrons/ (m^2 sec ster). The integral spectrum arising from cosmic ray interactions in the galaxy is also indicated.

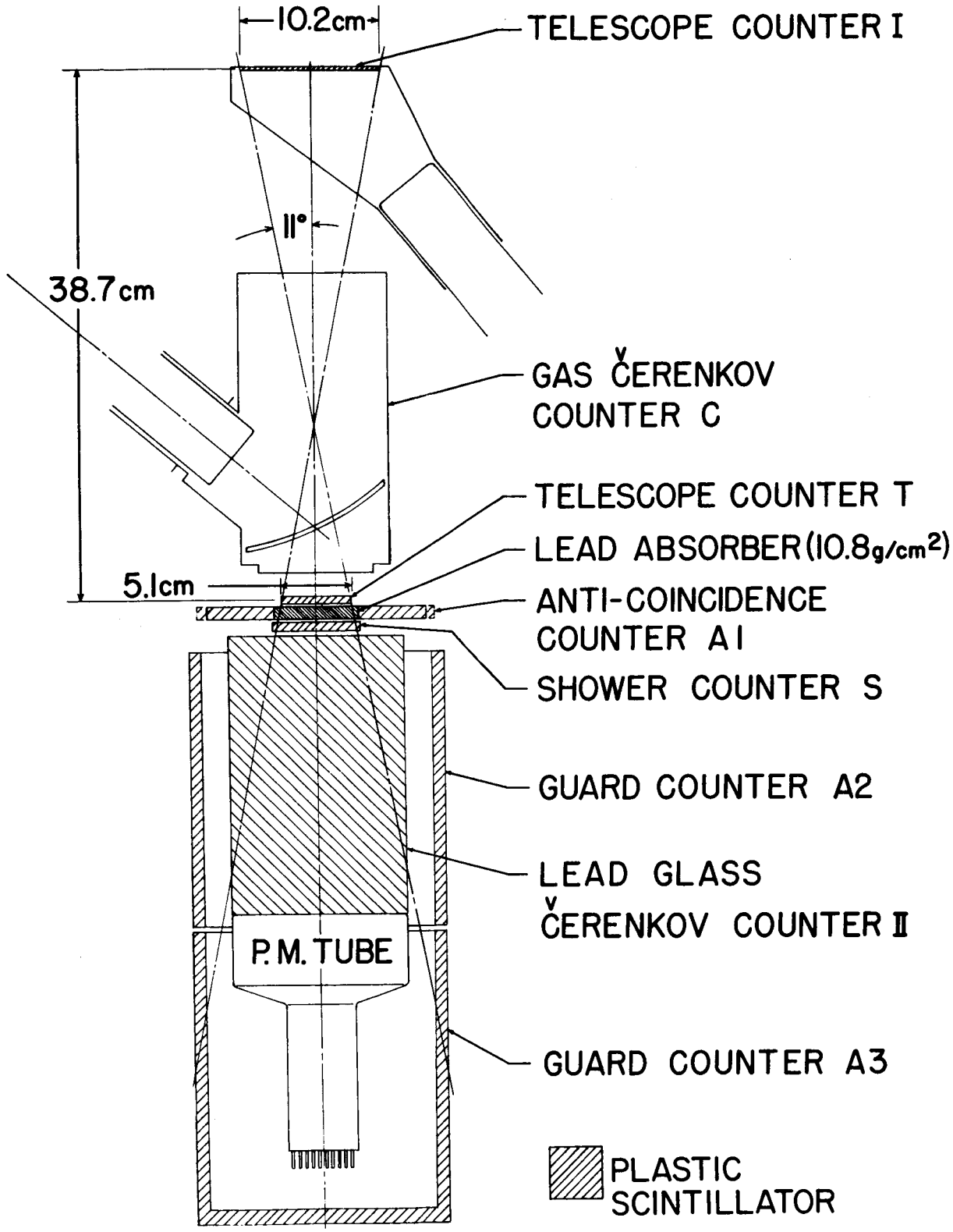
10.2cm
TELESCOPE COUNTER I
11°
38.7cm
GAS ČERENKOV
COUNTER C
TELESCOPE COUNTER T
LEAD ABSORBER (10.8g/cm²)
5.1cm
ANTI-COINCIDENCE
COUNTER A1
SHOWER COUNTER S
GUARD COUNTER A2
LEAD GLASS
ČERENKOV COUNTER II
P.M. TUBE
GUARD COUNTER A3
PLASTIC
SCINTILLATOR

Fig. 1

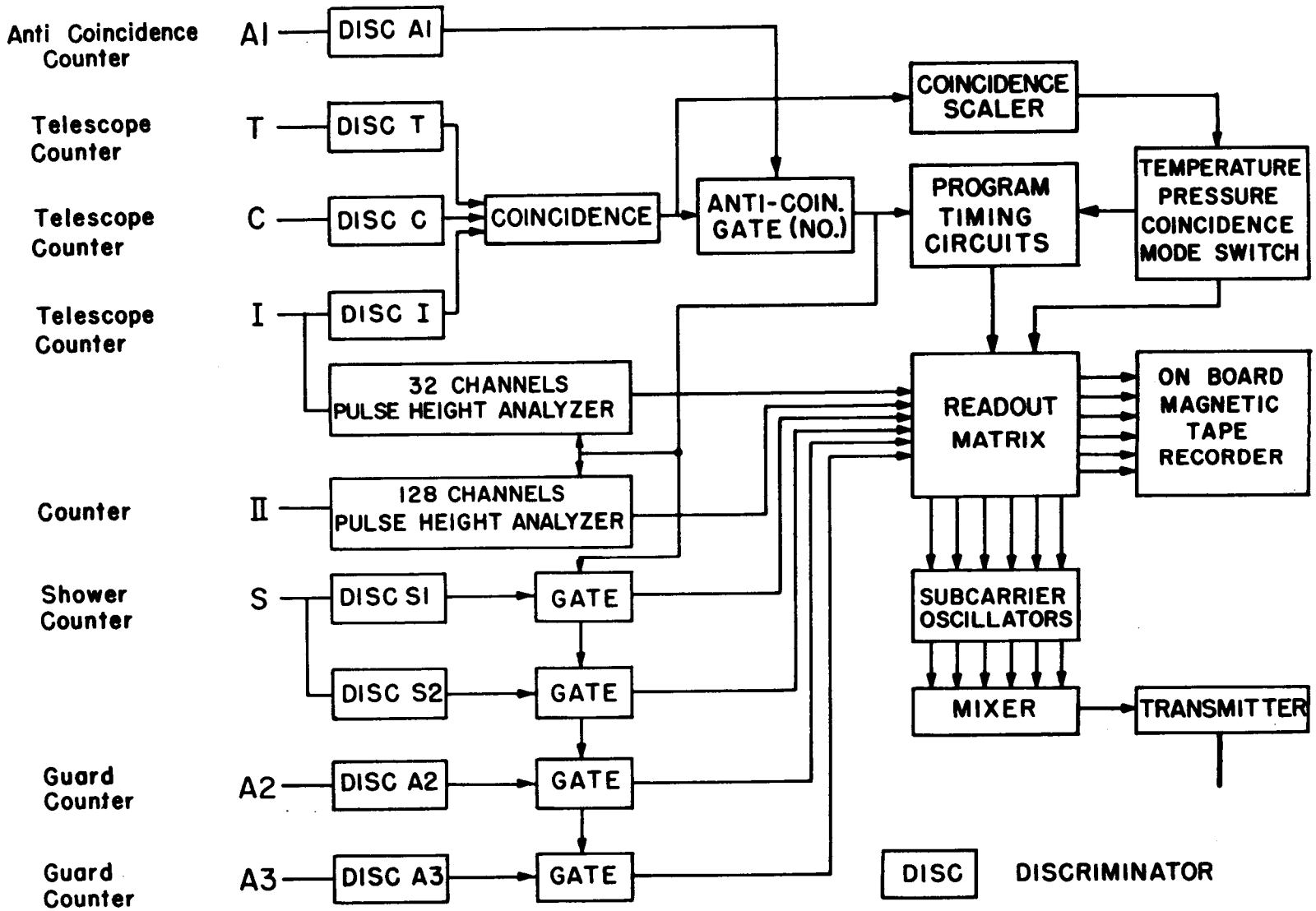
Anti Coincidence Counter
A1
DISC A1
Telescope Counter
T
DISC T
Telescope Counter
C
DISC C
COINCIDENCE
Telescope Counter
I
DISC I
ANTI-COIN. GATE (NO.)
COINCIDENCE SCALER
PROGRAM TIMING CIRCUITS
TEMPERATURE PRESSURE COINCIDENCE MODE SWITCH
32 CHANNELS PULSE HEIGHT ANALYZER
READOUT MATRIX
ON BOARD MAGNETIC TAPE RECORDER
Counter
II
128 CHANNELS PULSE HEIGHT ANALYZER
Shower Counter
S
DISC S1
GATE
SUBCARRIER OSCILLATORS
DISC S2
GATE
MIXER
TRANSMITTER
Guard Counter
A2
DISC A2
GATE
Guard Counter
A3
DISC A3
GATE
DISC
DISCRIMINATOR

Fig. 2

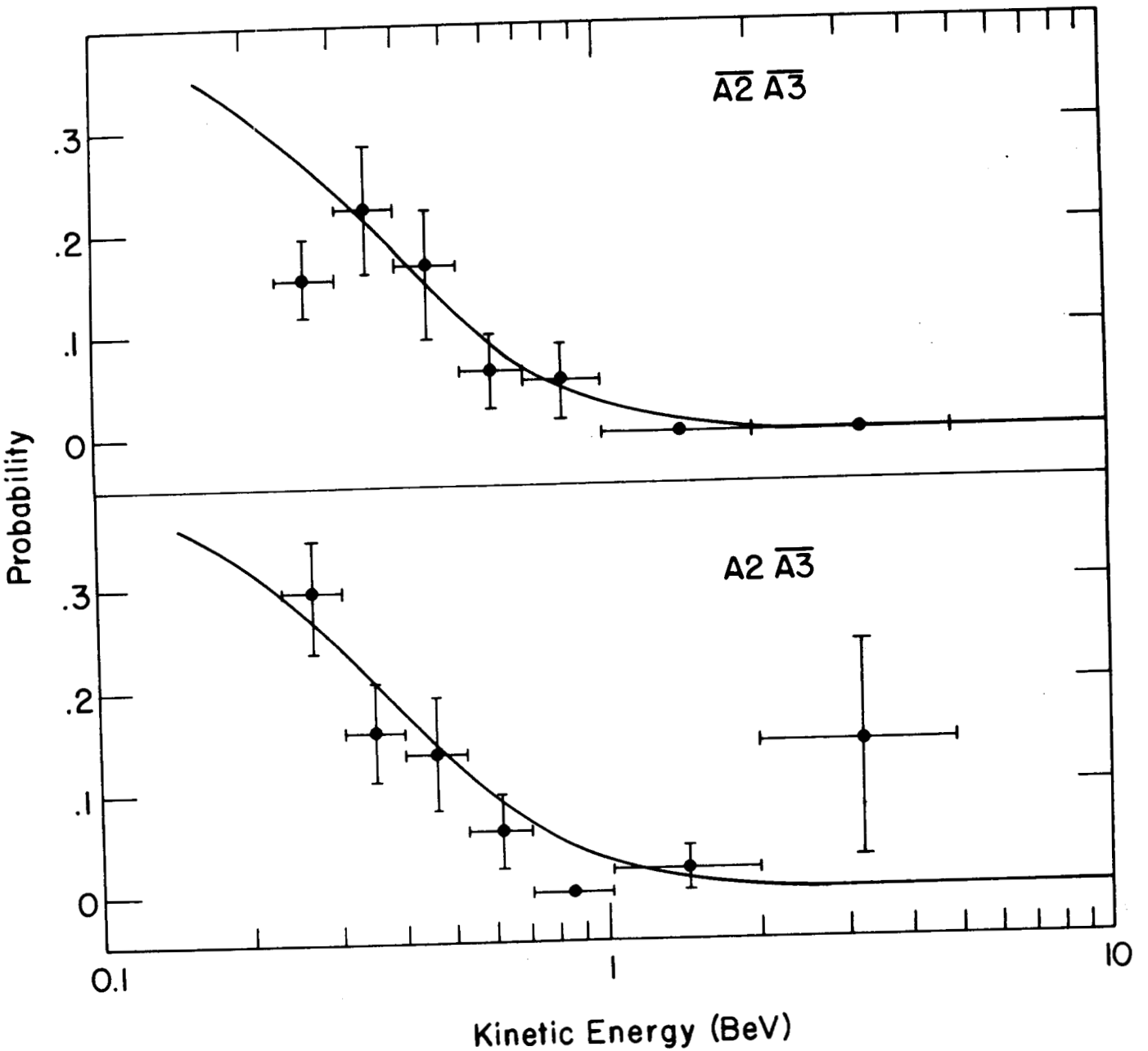
$\overline{A2}\ \overline{A3}$
$A2\ \overline{A3}$
Probability
.3
.2
.1
0
0.1
1
10
Kinetic Energy (BeV)

Fig. 3

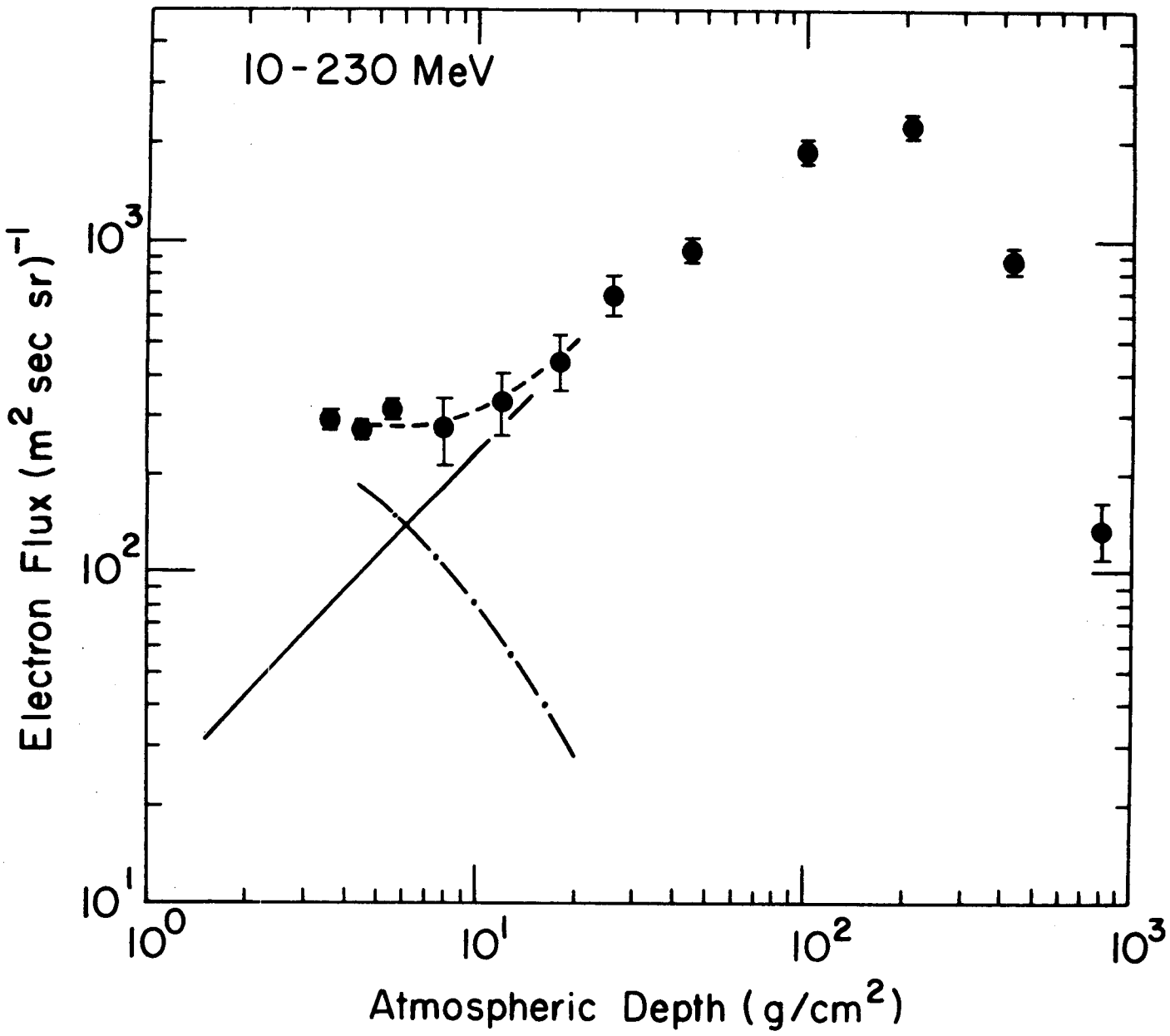
10-230 MeV
Electron Flux (m² sec sr)⁻¹
10³
10²
10¹
10⁰
10¹
10²
10³
Atmospheric Depth (g/cm²)

Fig. 4(a)

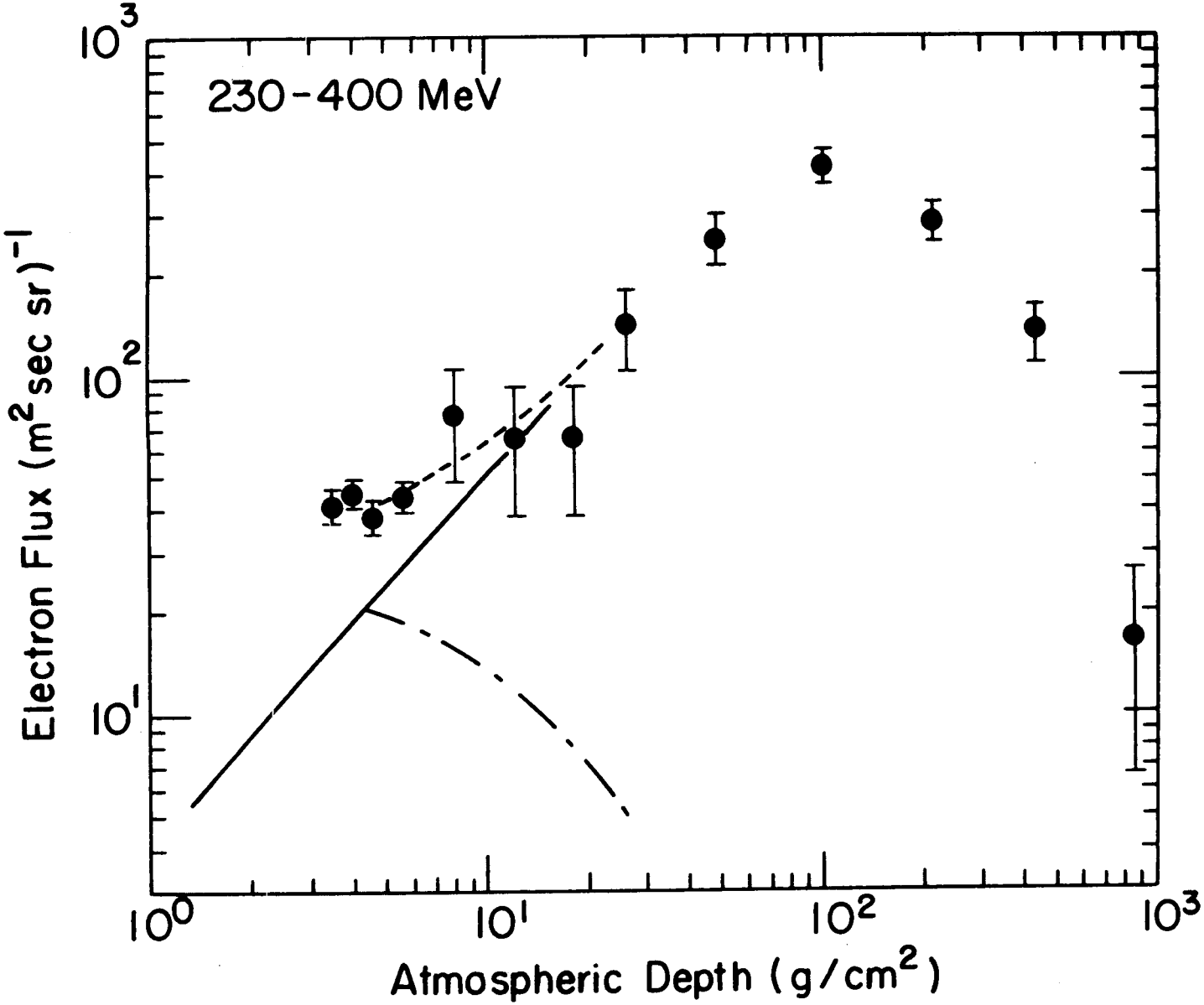
230-400 MeV
Electron Flux (m^2 sec sr)$^{-1}$
10^3
10^2
10^1
10^0
10^1
10^2
10^3
Atmospheric Depth (g/cm^2)

Fig. 4(b)

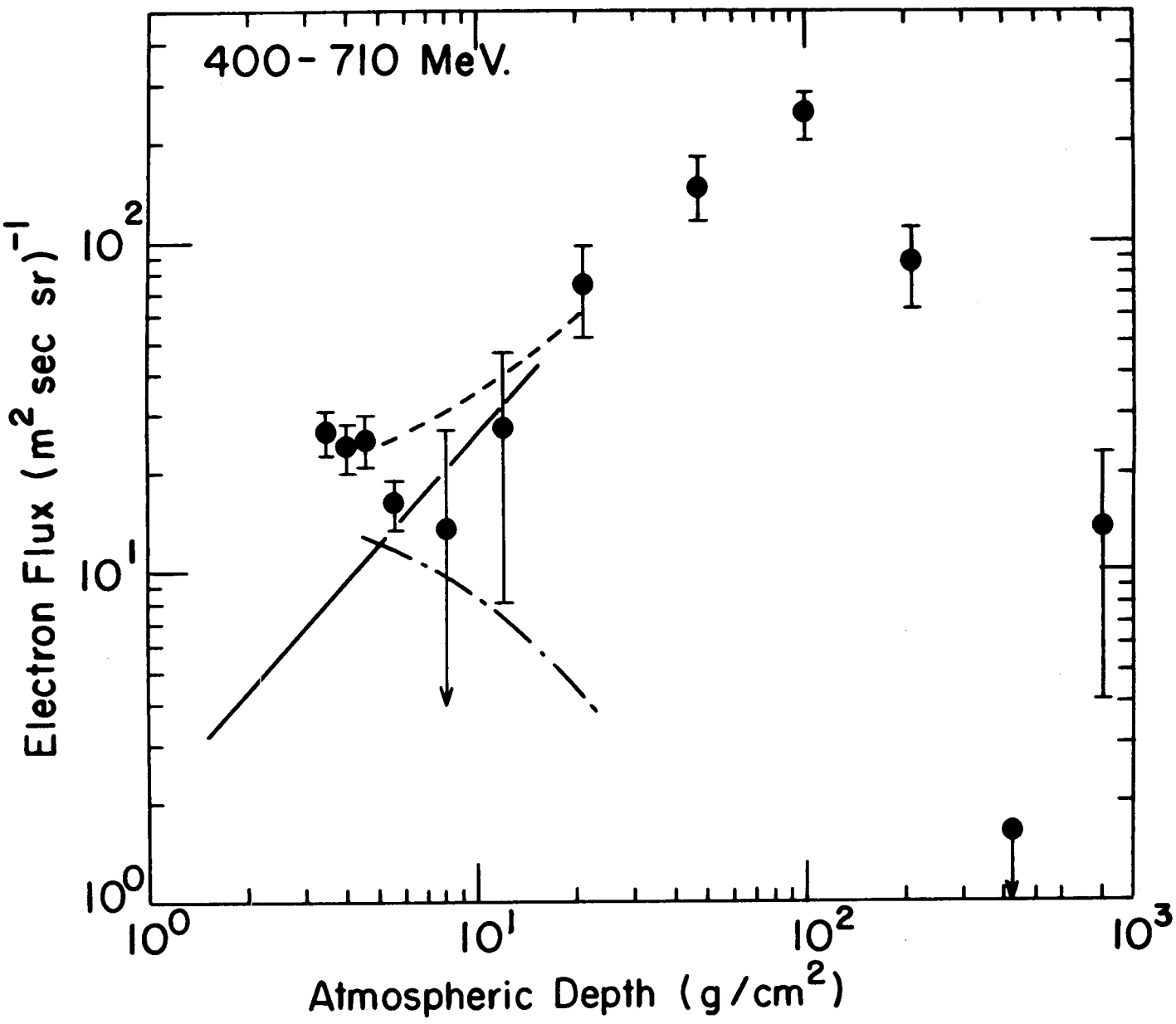
400 - 710 MeV.
Electron Flux (m² sec sr)⁻¹
10²
10¹
10⁰
10⁰
10¹
10²
10³
Atmospheric Depth (g/cm²)

Fig. 4(c)

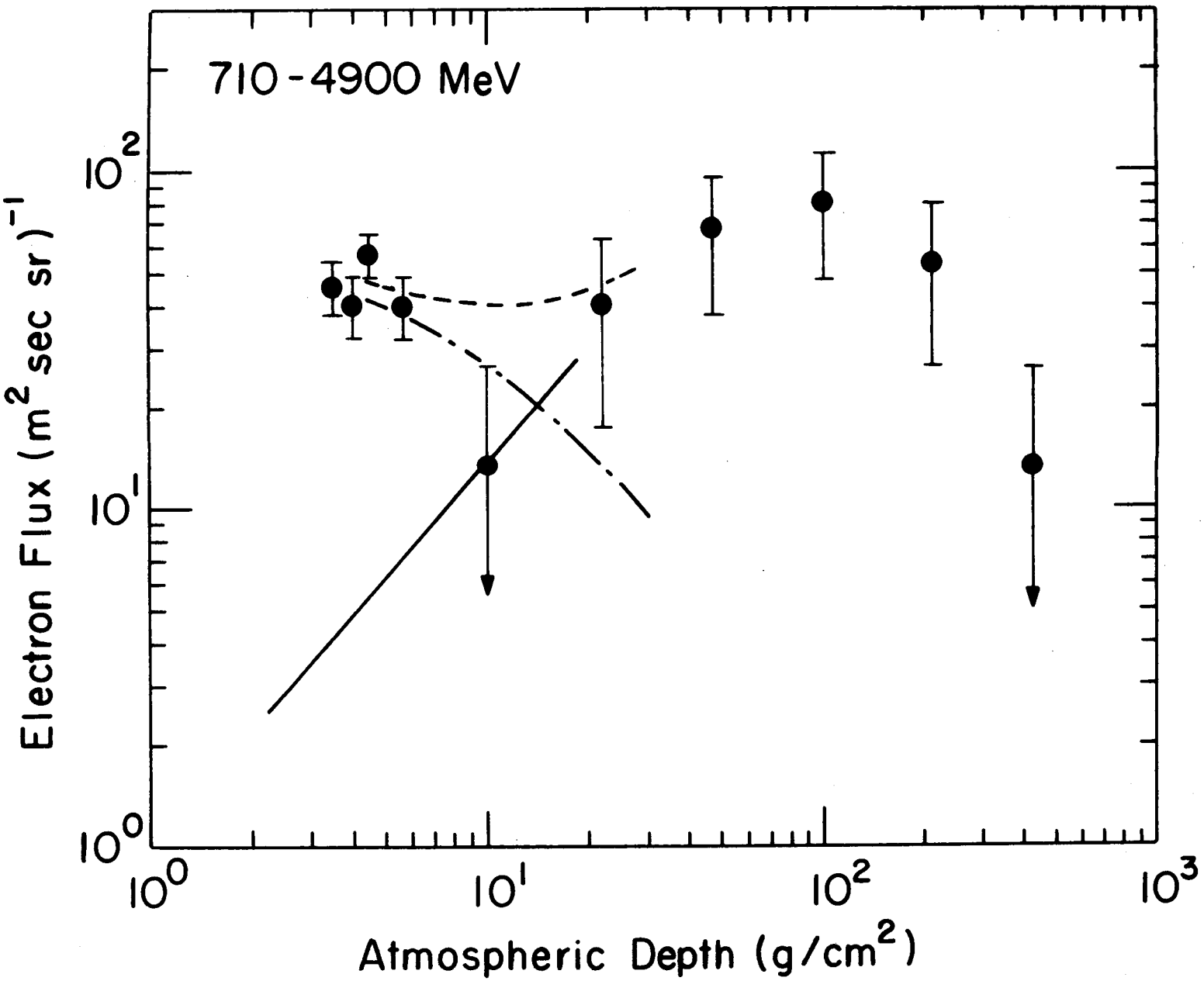
710 - 4900 MeV
Electron Flux (m^2 sec sr)$^{-1}$
10^2
10^1
10^0
10^0
10^1
10^2
10^3
Atmospheric Depth (g/cm^2)

Fig. 4(d)

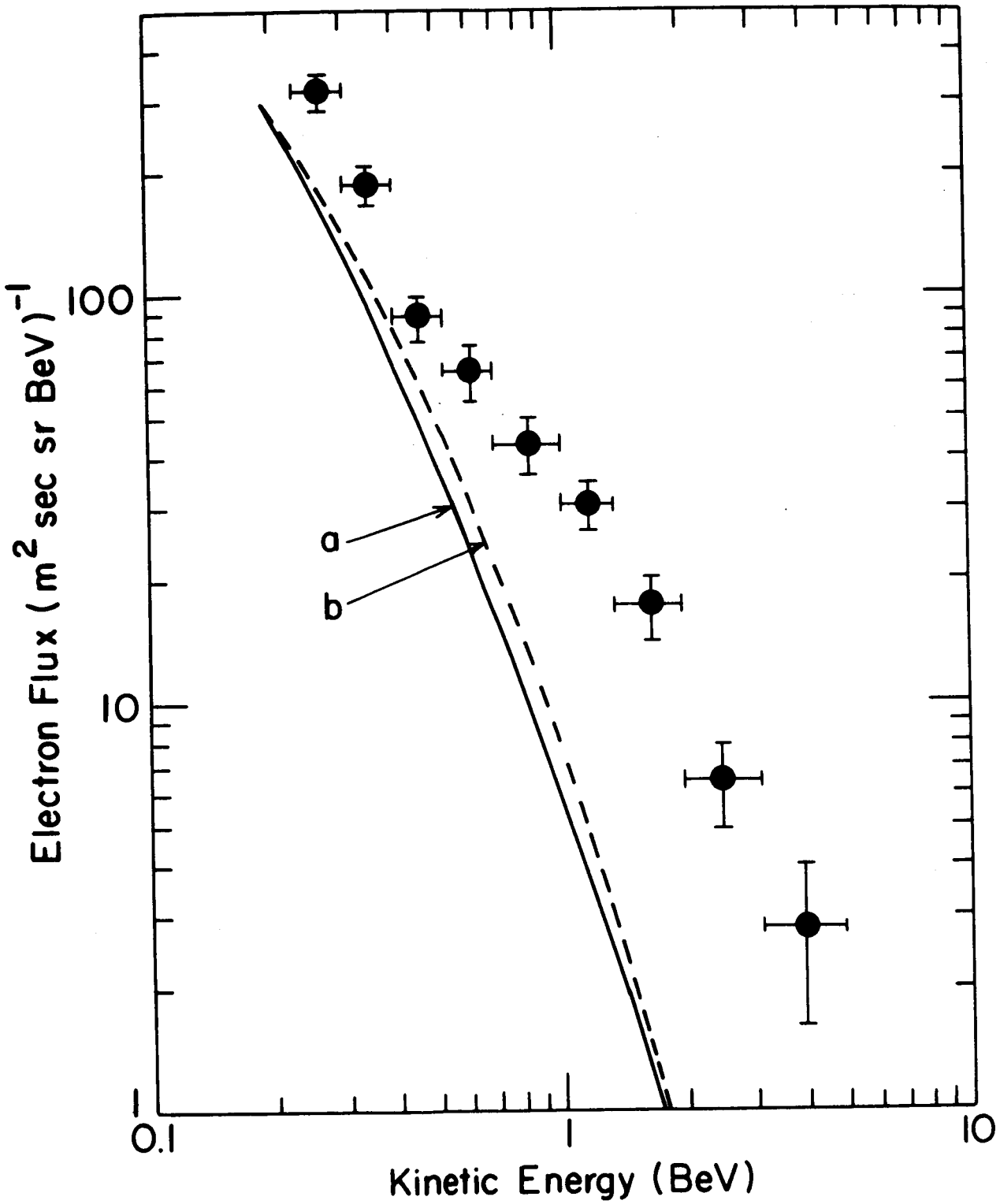
Electron Flux (m^2 sec sr BeV)$^{-1}$
100
10
1
0.1
1
10
Kinetic Energy (BeV)
a
b

Fig. 5

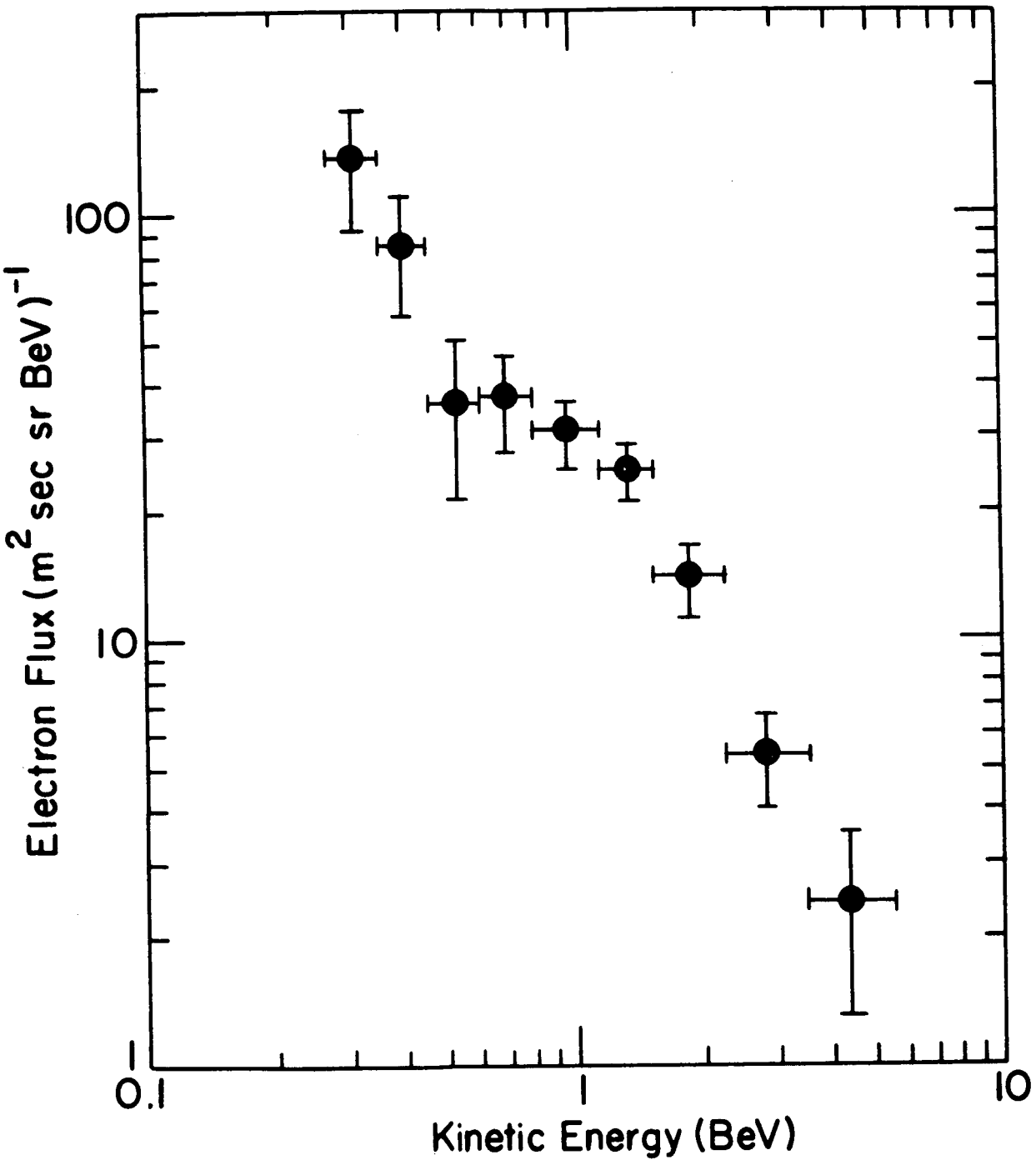
Electron Flux (m^2 sec sr BeV)$^{-1}$
100
10
1
0.1
1
10
Kinetic Energy (BeV)

Fig. 6

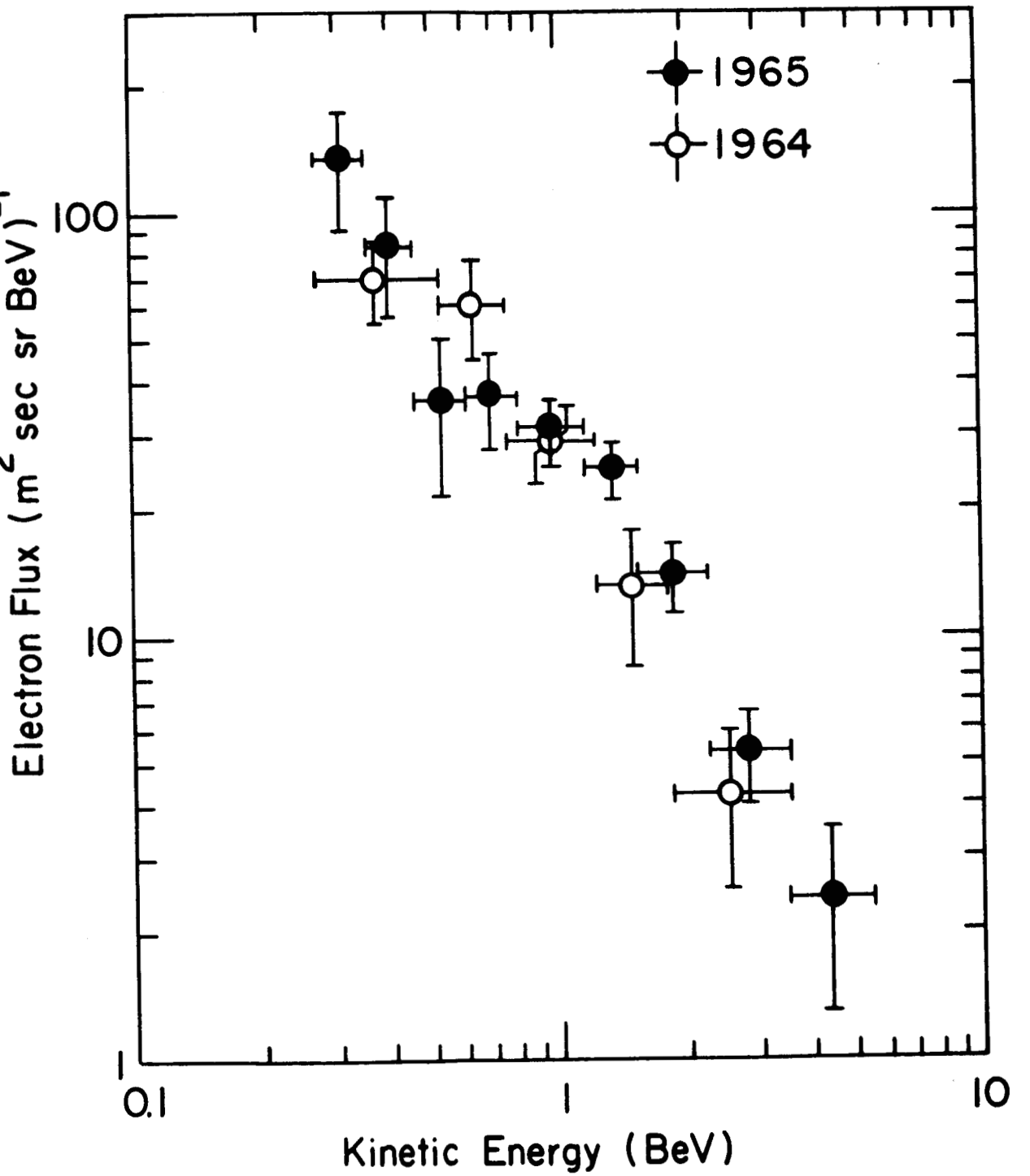
1965
1964
100
10
1
Electron Flux (m² sec sr BeV)⁻¹
0.1
1
10
Kinetic Energy (BeV)

Fig. 7

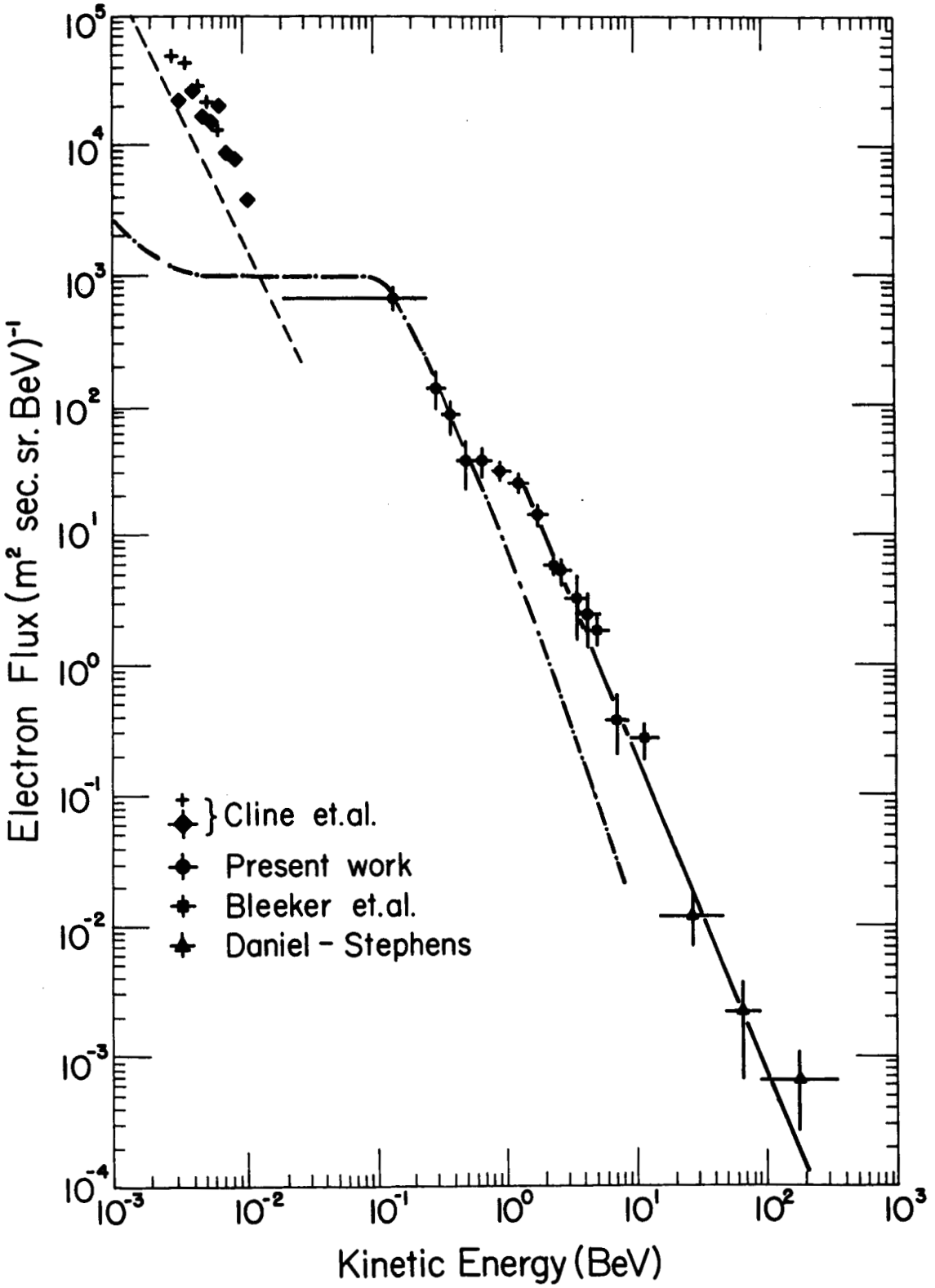
Electron Flux (m² sec. sr. BeV)⁻¹
Kinetic Energy (BeV)
Cline et.al.
Present work
Bleeker et.al.
Daniel - Stephens

Fig. 8

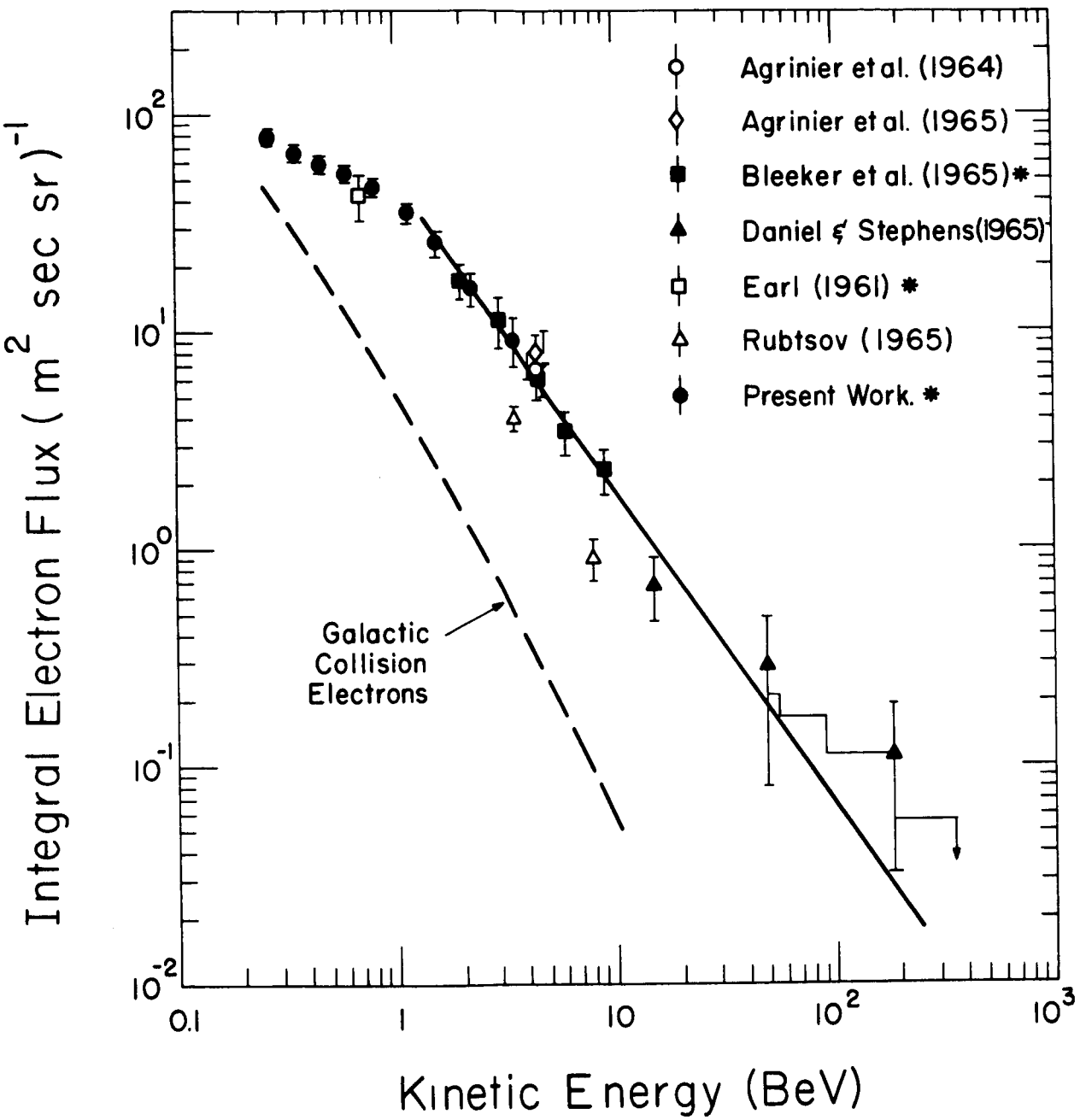
Agrinier et al. (1964)
Agrinier et al. (1965)
Bleeker et al. (1965)*
Daniel & Stephens(1965)
Earl (1961) *
Rubtsov (1965)
Present Work. *
Galactic
Collision
Electrons
Integral Electron Flux (m^2 sec sr)$^{-1}$
Kinetic Energy (BeV)
10^2
10^1
10^0
10^{-1}
10^{-2}
0.1
1
10
10^2
10^3

Fig. 9